Journal of Building Engineering 101 (2025) 111796

Contents lists available at ScienceDirect

Journal of Building Engineering

journal homepage: www.elsevier.com/locate/jobe

# Optimizing building energy efficiency: A precise BIM-Based approach for quantifying thermal bridges

Mergim Gaši [a,*], Domagoj Tkalčić [a], Bojan Milovanović [a], Mihaela Maslać [b]

[a] Faculty of Civil Engineering, University of Zagreb, Croatia
[b] MXM Architecture, Croatia

ARTICLE INFO

*Keywords:*
Thermal bridges
Linear thermal transmittance
Transmission heat losses
Numerical simulations
BIM model
Section method

ABSTRACT

Thermal bridges have a significant impact on the energy efficiency of buildings, but their accurate assessment remains a challenge. In this paper, a novel method for estimating the Ψ-values of thermal bridges and their contribution to the transmission heat losses ($H_{tr,TB}$) is proposed to solve this problem. The proposed method involves calculating the total heat flux across the building cross-sections and subtracting the 1D heat flux of the individual components to derive the Ψ-values. Horizontal and vertical cross-sections are extracted from a 3D BIM (Building Information Modelling) model in Archicad. Numerical simulations are carried out on these cross-sections, which represent the entire building envelope. The method was validated on two buildings: a simple building and a complex multi-part building. The results show that with only three cross-sections (one horizontal and two vertical) $H_{tr,TB}$ can be estimated with less than 2 % error compared to the standard numerical analysis method defined in EN ISO 10211, where each thermal bridge is calculated individually. The proposed method is faster and eliminates the need for manual identification and measurement of thermal bridges. This simplified approach achieves equivalent accuracy and is particularly beneficial for smaller projects. The study emphasises the potential of using BIM tools for practical, efficient thermal bridge analysis.

## 1. Introduction

Nearly Zero Energy Buildings (nZEB) are designed for very high energy performance, with the energy required coming largely from renewable sources generated on site or close to the building location. One of the biggest challenges in the realization of nZEB and ultimately in the transition to Zero-Emission Buildings (ZEB) is the effective management of thermal bridges, i.e. places in the building envelope where the heat flow is significantly higher than in the surrounding areas. Thermal bridges can lead to increased heat loss, condensation problems and lower overall energy efficiency of buildings [1]. Modern materials and construction techniques are used to mitigate these effects. For example, the use of high-performance insulation materials, thermal breaks and continuous insulation layers are key strategies for minimizing thermal bridges [2]. Building information modeling (BIM) also plays an important role in identifying and eliminating thermal bridges during the design phase and enables precise simulation and optimization of building components to effectively reduce heat loss [3]. The elimination of thermal bridges not only improves the energy efficiency of nZEBs but is also crucial for meeting the demanding performance criteria of ZEBs and ensures that the buildings contribute to sustainability goals and climate change mitigation [4]. The recast EU Energy Performance of Buildings Directive (EU/2024/1275) requires all new residential and

* Corresponding author.
*E-mail address:* mergim.gasi@grad.unizg.hr (M. Gaši).

https://doi.org/10.1016/j.jobe.2025.111796
Received 26 August 2024; Received in revised form 9 December 2024; Accepted 4 January 2025
Available online 9 January 2025

non-residential buildings to be ZEBs from 2028 (public buildings) or 2030 (all other buildings). This directive focuses on high energy performance and the use of renewable energy to achieve climate neutrality by 2050 [5].

The numerical calculations of thermal bridges can be performed using both two-dimensional (2D) and three-dimensional (3D) modeling approaches. While 2D models focus on cross-sections of building components and evaluate the linear thermal transmittance (Ψ-value), they cannot fully capture the complexity of thermal bridges at intersections and corners [6]. In contrast, 3D models offer a more comprehensive analysis by taking into account the full geometric and material complexity of the building elements and provide detailed insights into thermal bridging effects. Despite their accuracy, 3D models require considerable computational resources and detailed input data, which can limit their wide application [7].

Building Information Modeling (BIM) has proven to be a valuable tool for addressing these complexities. BIM integrates detailed geometry and material data into thermal simulations, improving the accuracy of 2D and 3D thermal bridge analysis. This integration enables the automation of thermal bridge identification and calculation, streamlining the design process and optimizing the energy performance of buildings from the early design stages [8]. In addition, BIM facilitates the implementation of advanced energy efficiency measures and ensures compliance with evolving energy regulations and standards [9].

Recent studies have shown that BIM-based approaches not only improve the accuracy of energy simulations, but also support comprehensive sustainability assessments. For example, Carvalho et al. [10] demonstrated the application of BIM for energy analysis and sustainability assessment in Portuguese buildings and showed how it can modernize the assessment of energy performance and support sustainable building practices. Similarly, Tkalčić et al. [11] investigated different insulation materials and configurations, such as Lightweight Steel Frame (LSF) walls with a 6-m span, demonstrating reductions of up to 67 % in heat transfer losses when optimized thermal bridge designs were employed. These findings underline the importance of detailed and accurate thermal bridge analysis in achieving nZEB and ZEB goals.

While previous studies have provided valuable insights, existing methods often require significant computational resources or rely on approximations that lack precision in capturing complex thermal bridge interactions. Moreover, there is a need for a streamlined methodology that balances computational efficiency with accuracy. This study addresses these challenges by introducing a simplified section method for assessing $H_{tr,TB}$ using BIM tools. The method reduces computational effort while maintaining accuracy, demonstrating its potential as a practical tool for thermal bridge analysis in energy-efficient buildings.

BIM is increasingly being used to integrate Building Energy Modeling (BEM) and Building Energy Simulation (BES) to improve the energy efficiency of buildings. Gao et al. [12] emphasize that BIM-based BEM overcomes traditional modeling limitations, improves consistency and reduces costs. Sanhudo et al. [13] investigate the role of BIM in energy retrofit and emphasize the possibilities of data collection and energy analysis. Vaz et al. [8] investigate the interoperability between BIM and BES and point out that the simplification of complex geometries improves data transfer, increasing simulation accuracy and energy performance.

Simplifications in thermal bridge calculations are often necessary to achieve a balance between accuracy and calculation efficiency. Common approaches to these simplifications include the use of thermal bridge atlases or predefined Ψ-values from standards, which provide quick estimates but may not offer the precision of detailed simulations. Designers often struggle with the absence of representative details in thermal bridge atlases. Numerical calculations, while accurate, require significant time and resources. It is essential for both atlases and numerical methods to focus on construction details that have the most significant impact on the building physics design. Although there is a growing appreciation for the importance of thermal bridges among engineers and architects, they often lack the time to thoroughly address them.

It is crucial to emphasize the role of designers' expertise in identifying and prioritizing thermal bridges that require detailed analysis. Studies have shown that there is still a knowledge gap and lack of skills among designers regarding thermal bridges. Surveys indicate that many engineers and architects do not fully understand where or when thermal bridges occur. This lack of understanding is concerning because if a junction is not recognized as a potential thermal bridge, it may not be investigated, leading to substantial errors in energy calculations and the sizing of heating and cooling systems [14].

Comparative studies have evaluated the effectiveness of both simplified and detailed modeling techniques in assessing thermal bridges. For instance, dynamic analysis methods integrated with BIM environments have been shown to enable more accurate and efficient energy simulations [15]. Experimental methods such as the guarded hot box and numerical simulations have been used to determine the thermal transmittance of Lightweight Steel Frame (LSF) walls, emphasizing the significant influence of point thermal bridges [16–18]. Santos et al. [19,20] demonstrated that optimized configurations of LSF walls and detailed analyses are critical for achieving accurate energy efficiency assessments. Tkalčić et al. [11] showed that the use of advanced materials and design strategies, such as PVC spacers, can reduce heat transfer losses by up to 67 % in extreme cases. These findings highlight the importance of effective thermal bridge management in achieving energy-efficient building designs.

This study introduces a novel BIM-based method for calculating Ψ-values and total transmission heat losses ($H_{tr,TB}$) of thermal bridges using a simplified section method. The primary objectives of this research are: (1) to compare the accuracy and efficiency of the section method with the standardized EN ISO 10211 approach, and (2) to demonstrate that the section method can reliably approximate $H_{tr,TB}$ using only three cross-sections (one horizontal and two vertical). By leveraging BIM tools to streamline cross-section extraction and thermal analysis, the section method is shown to achieve a high level of accuracy (less than 2 % error) with significantly reduced computational effort. These results highlight the practical advantages of the section method in optimizing thermal bridge analysis for highly energy-efficient buildings.

**Table 1**
Table of variables.

| Variable | Definition | Units |
|---|---|---|
| $\Psi_{H,j}$ | Linear thermal transmittance in the horizontal direction | W/m·K |
| $\Psi_{V,j}$ | Linear thermal transmittance in the vertical direction | W/m·K |
| $\Psi_{U,j}$ | Linear thermal transmittance in the perpendicular vertical direction | W/m·K |
| $\Psi_{avg,H}$ | Average linear thermal transmittance for horizontal cross-sections | W/m·K |
| $\Psi_{avg,V}$ | Average linear thermal transmittance for vertical cross-sections | W/m·K |
| $\Psi_{avg,U}$ | Average linear thermal transmittance for perpendicular vertical cross-sections | W/m·K |
| $L_{2D}$ | Thermal coupling coefficient, total heat transfer across a 2D surface | W/m·K |
| $L_{2D,eq,H}$ | Equivalent thermal coupling coefficient for horizontal cross-sections | W/m·K |
| $L_{2D,eq,V}$ | Equivalent thermal coupling coefficient for vertical cross-sections | W/m·K |
| $L_{2D,eq,U}$ | Equivalent thermal coupling coefficient for perpendicular vertical cross-sections | W/m·K |
| $U_i$ | Thermal transmittance of 1D building elements (walls, slabs, windows, etc.) | W/m$^2$·K |
| $L_i$ | Length of a 1D element (extent of the thermal bridge) | m |
| $H_{tr}$ | Total transmission heat losses | W/K |
| $H_{tr,TB}$ | Total transmission heat losses due to thermal bridges | W/K |
| $L_H$ | Total building height | m |
| $L_V$, $L_U$ | Total building lengths in two horizontal dimensions | m |
| $w_i$ | Weighting factor for each thermal bridge's contribution to Htr,TBH_{tr,TB}Htr,TB | % |
| $T_{int}$ | Indoor temperature | °C |
| $T_{ext}$ | Outdoor temperature | °C |
| $h_{in}$ | Indoor surface heat transfer coefficient | W/m$^2$·K |
| $h_{ex}$ | Outdoor surface heat transfer coefficient | W/m$^2$·K |
| $L_{max}$ | Length of the longest thermal bridge in a cross-section | m |
| $\Psi_{Lmax}$ | Linear transmittance of the longest thermal bridge in a cross-section | W/m·K |

## 2. Methodology

Accurately approximating total transmission heat losses in buildings due to thermal bridges ($H_{tr,TB}$) typically requires complex numerical calculations. These calculations are often limited to a small number of thermal bridges, providing only partial insight into the total transmission heat losses. This study addresses this limitation by introducing a simplified methodology for evaluating $H_{tr,TB}$ through the analysis of entire building cross-sections, reducing the need for extensive and time-consuming numerical calculations. This approach aims to bridge the knowledge gap in quantifying the impact of thermal bridges by considering the entire building envelope.

This research introduces a simplified formulation for calculating the thermal performance of the entire building using the building's cross-sections, referred to as the section method. This formulation isolates thermal bridge contributions by combining thermal coupling coefficients, linear thermal transmittance, and building dimensions for the calculation of $H_{tr,TB}$.

The research follows a structured methodology, as illustrated in Fig. 1, with the following steps.

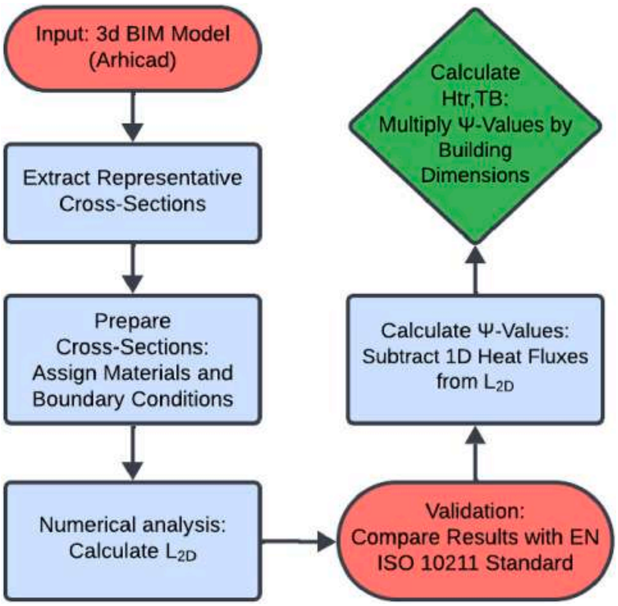


**Fig. 1.** Methodology flowchart.

1. Selection of Representative Cross-Sections

Horizontal and vertical cross-sections are extracted from a 3D BIM model using Archicad. For validation, two buildings were analyzed.

- o **EnergyPlus BESTTEST 960 (simple building)** [22]**:** A test case with six cross-sections (two horizontal and four vertical).
- o **Multi-Section Building:** A more complex building with 32 cross-sections. The cross-sections were chosen to represent the geometric characteristics of the buildings, approximating the 3D BIM model with 2D sections.

2. Preparation of Cross-Sections

The selected cross-sections were processed for thermal bridge analysis by assigning material properties and boundary conditions. Modern BIM tools (e.g., Archicad) simplify the extraction process, ensuring efficiency.

3. Numerical Calculations of Thermal Coupling Coefficients ($L_{2D}$)

Thermal bridge analysis was conducted using CRORAL software [21]. The results of numerical calculations for each cross-section were $L_{2D}$, which represents the thermal coupling coefficient.

4. Calculation of Ψ-Values

Using the equation below, the Ψ-values for vertical ($\Psi_H$) and horizontal ($\Psi_V$, $\Psi_U$) directions were calculated by subtracting the 1D heat fluxes ($\sum U_i \times L_i$) from $L_{2D}$:

$$\Psi_{H,j} = L_{2D} - \sum_i (U_i \cdot L_i)\Big|_{j=1\ to\ N_H}$$

$$\Psi_{V,j} = L_{2D} - \sum_i (U_i \cdot L_i)\Big|_{j=1\ to\ N_V}$$

$$\Psi_{U,j} = L_{2D} - \sum_i (U_i \cdot L_i)\Big|_{j=1\ to\ N_U} \quad (1)$$

5. Calculation of Transmission Heat Losses ($H_{tr,TB}$)

The calculated Ψ-values were multiplied by the main building dimensions ($L_H$, $L_V$, $L_U$) to estimate $H_{tr,TB}$, representing transmission heat losses due to thermal bridges.

6. Validation and Comparison

To validate the proposed method (referred to as the Section Method), results were compared to those obtained using the classical approach outlined in EN ISO 10211. The classical method involves detailed numerical analysis of all thermal bridges and manual identification of bridge lengths.

### *2.1. Key outcomes*

The Section Method demonstrated its capability to approximate $H_{tr,TB}$ with a minimal number of cross-sections, achieving less than 2 % error. Compared to the EN ISO 10211 standard [22], the proposed method eliminates the need for exhaustive thermal bridge identification and provides a streamlined, cost-effective alternative for practical applications.

### *2.2. Bridging the knowledge gap*

This research addresses the challenge of balancing accuracy and efficiency in thermal bridge calculations. By leveraging BIM tools and focusing on representative cross-sections, the Section Method offers a novel approach to simplifying the evaluation of transmission heat losses without compromising precision.

The variables used in the calculations are defined in Table 1. This table provides a detailed explanation of each symbol, its physical meaning, and its units.

### *2.3. Creating cross-sections*

The cross-sections were exported from the 3D Archicad BIM model (Fig. 2). These cross-sections were generated at each point where the geometry or material changed. A total of 6 cross-sections were created for a simple building model (Fig. 3), while 32 cross-sections were required for a multi-section building model (Fig. 4). In Fig. 4, horizontal cross-sections are labeled as "HXXX," where "XXX" represents the cross-section number (e.g., "H001″). Vertical cross-sections are labeled as "UXX" and "VXX," with "XX" also representing the cross-section number (e.g., "U01" and "V01"). This stage is crucial as it is necessary to capture all thermal bridges in each cross-section in order to determine the minimal cross-sections required for accurate estimation of the effect of thermal bridges on total transmission heat losses.

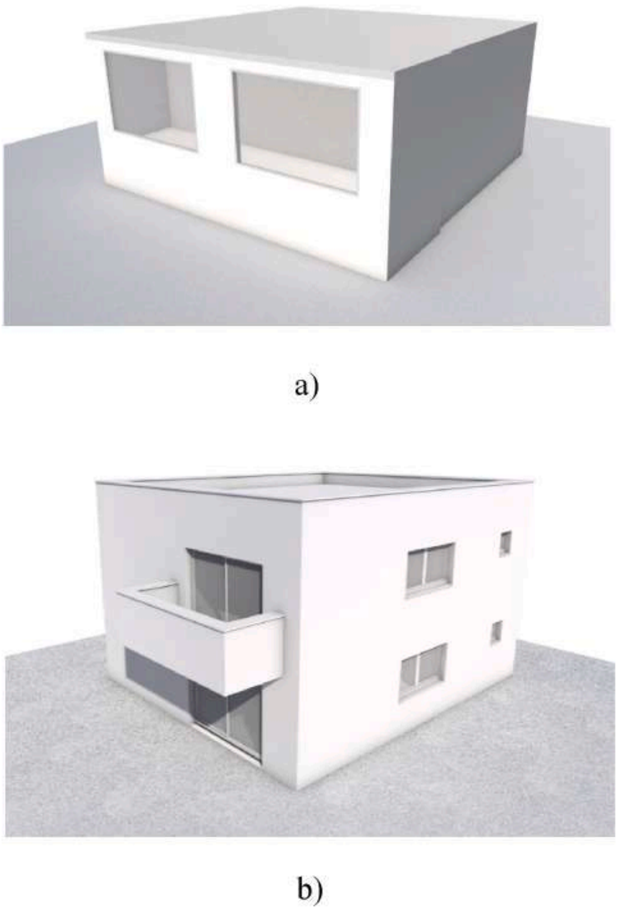


**Fig. 2.** Archicad 3D models; a) simple building, b) multi-section building.

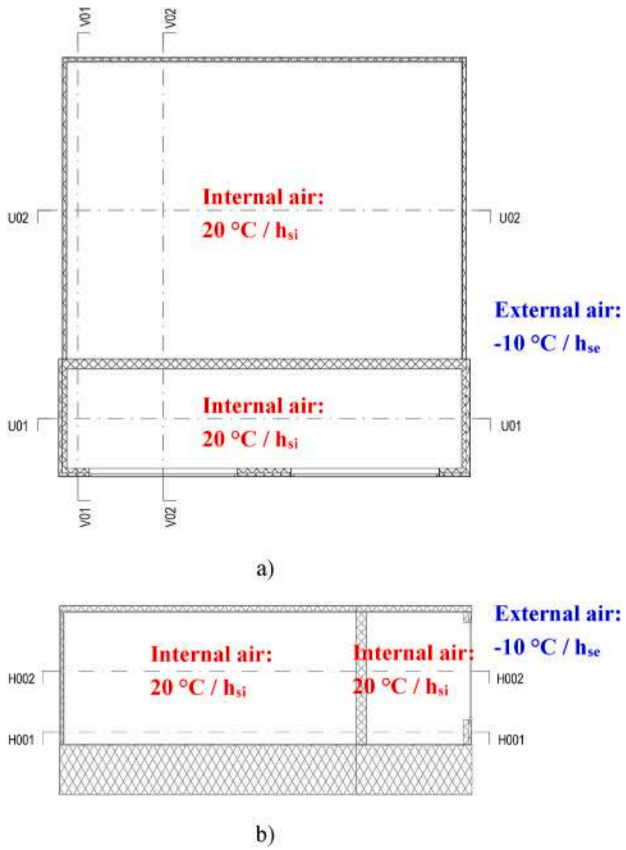


**Fig. 3.** Simple building cross-section locations; a) vertical and b) horizontal.

## 2.4. Numerical analysis

Numerical analysis was conducted using CRORAL, a software specialized in analyzing thermal bridges. CRORAL employs the Control Volume Method (CVM) for solving the heat equation, which discretizes the domain into control volumes and ensures energy conservation within each volume. This method is computationally efficient and well-suited for modeling complex thermal bridge geometries.

The analysis was based on cross-sections extracted from a 3D BIM model in Archicad. These cross-sections were transformed for compatibility with CRORAL to ensure seamless integration into the software. The results of the numerical analysis included detailed temperature data, which was used to calculate the thermal coupling coefficients ($L_{2D}$) for each cross-section. The analysis followed these steps.

1. **Import Transformed Files:** Transformed cross-section files exported from Archicad were imported into CRORAL.
2. **Apply Boundary Conditions and Material Properties:** Surface heat transfer coefficients, as detailed in Table 4, and material thermal properties were assigned to simulate realistic building conditions Table 3.
3. **Calculate Thermal Coupling Coefficient ($L_{2D}$):** Using the boundary conditions and material properties, coefficient $L_{2D}$ are calculated, which quantifies the total heat transfer for a cross-section.
4. **Calculate Ψ-Values:** The linear thermal transmittance (Ψ) was calculated by subtracting the sum of all 1D transmission heat losses (ΣUi·Li) from the thermal coupling coefficient ($L_{2D}$) for each cross-section. Fig. 5 provides an example of this calculation.
5. **Repeat Calculations for All Dimensions:** The procedure was repeated for all cross-sections in the three primary building dimensions: height ($L_H$) and two lengths ($L_V$ and $L_U$).

The heat source in this analysis was a constant temperature gradient applied across the building envelope, simulating indoor and outdoor conditions of 20 °C and −10 °C, respectively. These temperatures represent typical winter conditions for evaluating heat losses in the building. The chosen gradient reflects real-world scenarios where thermal bridges play a significant role in heat transfer.

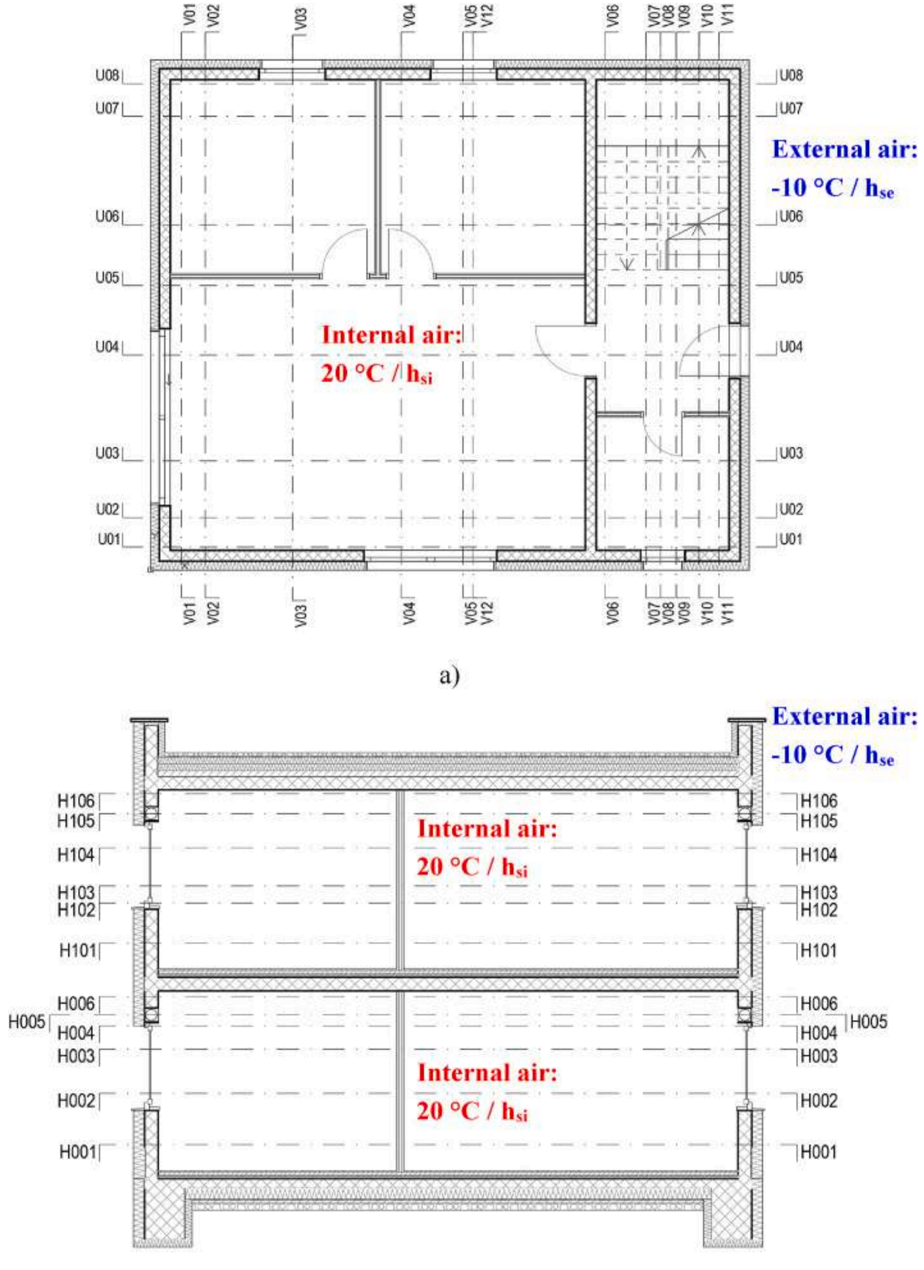


**Fig. 4.** Multi-section building cross-section locations; a) vertical and b) horizontal.

When calculating the 1D transmission heat losses, it was crucial to use the exact dimensions from the building physics design to ensure consistency and accuracy. By aligning the dimensions, potential inconsistencies that might arise from mismatched measurements were eliminated, maintaining the integrity of the thermal analysis.

The final results of the numerical analysis were used to estimate the total transmission heat losses due to thermal bridges ($H_{tr,TB}$) for the building. These results were validated by comparing the section method with the EN ISO 10211 approach. Errors were calculated as the percentage difference between the two methods, providing insight into the accuracy and computational efficiency of the proposed approach.

**Table 2**
Material characteristics for a simple building.

| Material name | Thermal conductivity λ [W/(m K) |
|---|---|
| Plasterboard | 0.160 |
| Fiberglass Quilt | 0.040 |
| Wood Siding | 0.140 |
| Roof Deck | 0.140 |
| Timber Flooring | 0.140 |
| Insulation | 0.040 |
| Common Wall | 0.510 |

**Table 3**
Material characteristics for a multi-section building.

| Material name | Thermal conductivity λ [W/(m K) |
|---|---|
| Mineral wool | 0.035 |
| Reinforced concrete | 2.600 |
| Extruded polystyrene (XPS) | 0.035 |
| Gravel | 2.000 |
| Concrete | 2.000 |
| Screed | 1.600 |
| Expanded polystyrene (EPS) | 0.040 |
| Ceramic tiles | 1.300 |
| Parquet | 0.150 |
| Shutter box | 0.600 |
| Polyurethane foam | 0.023 |
| Window | 0.130 |
| Plasterboard | 0.250 |

**Table 4**
Boundary conditions.

| Material name | Surface heat transfer coefficient h [W/(m$^2$ K)] |
|---|---|
| Interior (horizontal) | 7.69 |
| Interior (upwards) | 10.00 |
| Interior (downwards) | 5.88 |
| Exterior | 25.00 |

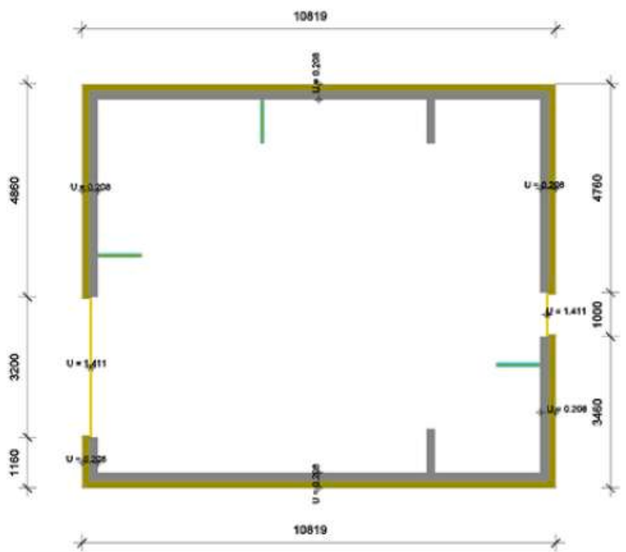


**Fig. 5.** 1D transmission heat losses (U-values and dimensions in milimeters).

### 2.4.1. Material characteristics and boundary conditions

The material properties are listed in Tables 2 and 3. The boundary conditions derived from EN ISO 9469 [23] (Table 4) depend on the environment (internal and external) and the direction of heat flow (horizontal, upward or downward). These conditions were applied uniformly across all modeled elements unless otherwise stated. The surface heat transfer coefficients (h) represent the rate of heat transfer per unit area due to conduction, convection, and radiation at the interior and exterior surfaces of the building elements. Interior boundaries, such as those separating conditioned spaces, were treated so the temperature between those spaces is equal and no heat is moving through those boundaries. Interior boundaries separating external and internal environment were modeled using a constant temperature of the interior air and heat transfer coefficient (h) for internal surfaces given in ISO 9469 (Table 4). External surface were modeled the same way as the internal surfaces but with heat transfer coefficient h for external surfaces (Table 4). Cutt-off planes (internal walls, floors, etc.) were modeled as adiabatic surfaces. The values of the internal and external temperatures are not important because unit temperature difference (1 K) is sufficient for calculating heat losses. The ground was not modeled, but an external boundary condition below the foundation was applied. This simplification was made as the focus of this work is to show the differences between the classical numerical analysis of thermal bridges and the approach presented here. However, if detailed ground modeling is required, as specified in EN ISO 10211 and EN ISO 13786 [24], the same approach as described in this paper can be applied. An additional approximation was applied to windows and doors, modeling them as a homogeneous material with uniform thermal conductivity and thickness. This approach is considered acceptable by Schild [25] in situations where specific window properties are unavailable during the design phase.

Typical building elements and their thicknesses are shown in Figs. 6 and 7.

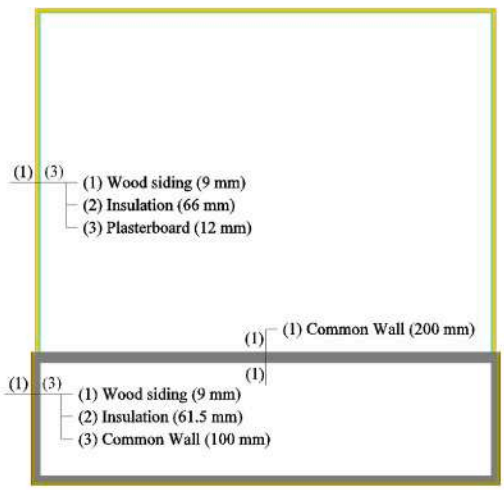


a)

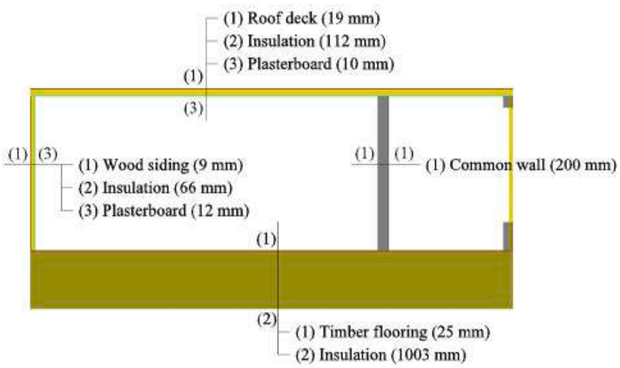


b)

**Fig. 6.** Simple building's element thicknesses; a) horizontal, b) vertical.

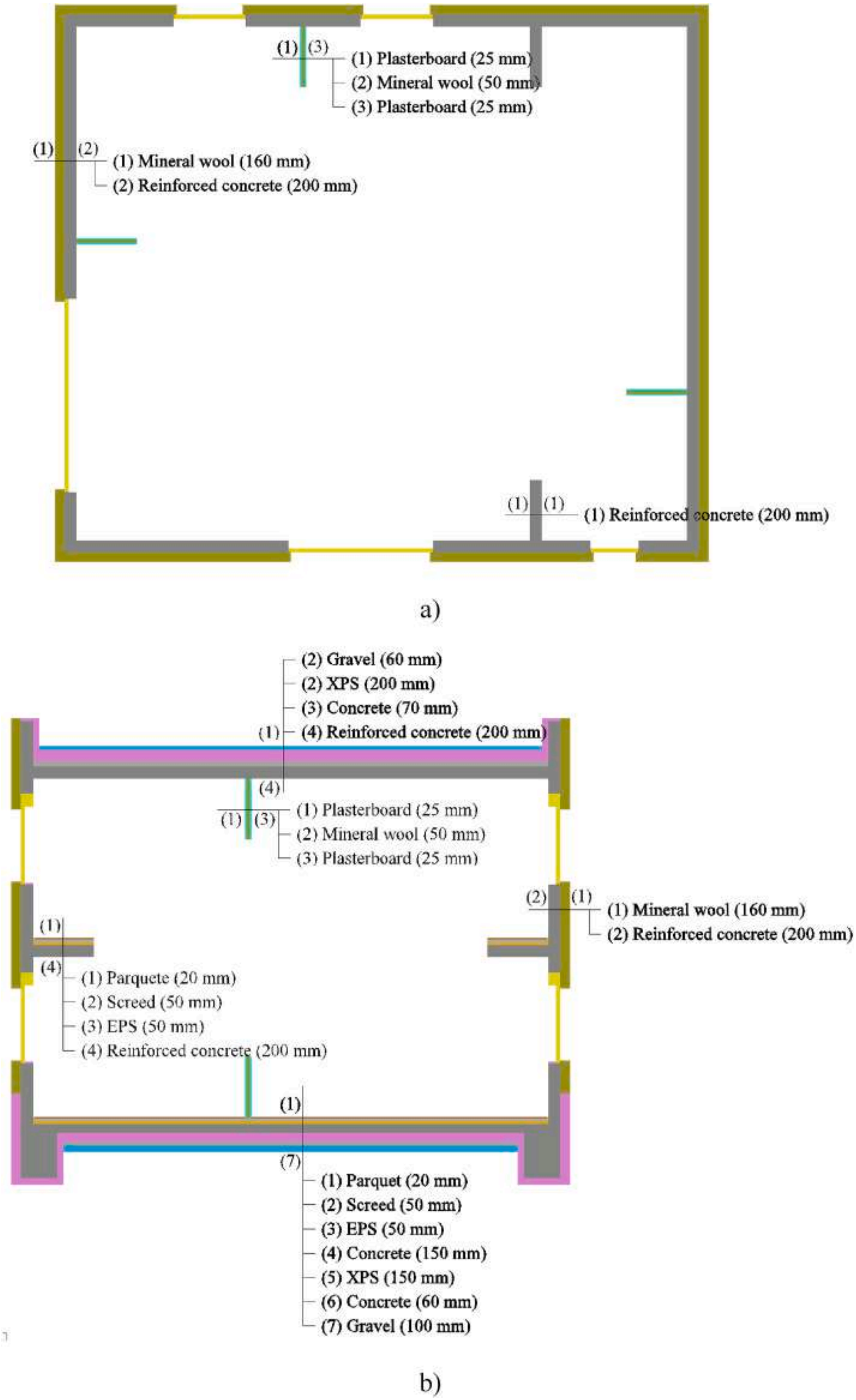


**Fig. 7.** Multi-section building's element thicknesses; a) horizontal, b) vertical.

## 3. Results

This study compares two methods for calculating the Ψ-values of thermal bridges: the section method described in this paper and the standardized approach described in EN ISO 10211.

### 3.1. Section method

The approach presented in this paper can be used to approximate the real 3D heat flux by creating horizontal (H) and vertical (V and U) sections. The best approximation is achieved when all sections are used (Fig. 8).

Fig. 8 presents the temperature distribution obtained from the numerical analysis of the multi-section building. This distribution, calculated for each of the 32 cross-sections shown in Fig. 3, is critical for estimating the heat flux through thermal bridges. The cross-sections were extended along their corresponding lengths to reconstruct the building's 3D geometry, allowing for an accurate approximation of actual 3D heat losses. The figure highlights higher temperature gradients at junctions and corners, indicating significant heat loss through these areas. These findings demonstrate the section method's ability to capture the thermal behavior of the building envelope, aligning with the research objective of simplifying and improving the accuracy of thermal bridge analysis.

Figs. 9 and 10 show the Ψ-values calculated for the cross-sections of a simple building and a multi-section building, respectively. These values quantify the linear heat transfer characteristics of thermal bridges across the three primary dimensions: height ($L_H$) and lengths ($L_V$, $L_U$). The average Ψ-values ($\Psi_{avg}$) provide a straightforward comparison of Ψ-values across all cross-sections, revealing their overall variability. In contrast, the equivalent Ψ-values ($\Psi_{eq}$), calculated using Equation (2), normalize these values to the building dimensions, enabling a proportional analysis of heat transfer contributions.

For the simple building, the Ψ-values are relatively consistent across cross-sections, reflecting its simpler geometry. Equally, the multi-section building exhibits greater variability, particularly in vertical sections, due to its more complex structure and material interactions. These findings demonstrate the section method's ability to capture the thermal behavior of building envelopes while maintaining accuracy, even for more geometrically complex buildings. The Ψ-values shown in these figures form the basis for calculating total heat losses ($H_{tr,TB}$), validating the research objective of providing an efficient alternative to the EN ISO 10211 method.

$$\Psi_{eq,H} = \frac{\sum_i (\Psi_{H_i})}{L_H}$$

$$\Psi_{eq,V} = \frac{\sum_j (\Psi_{V_j})}{L_V}$$

$$\Psi_{eq,U} = \frac{\sum_k (\Psi_{U_k})}{L_U} \tag{2}$$

After calculating the Ψ-values, it is possible to calculate the $H_{tr,TB}$ by multiplying the Ψ-values by the corresponding lengths – Eq (2).

$$H_{tr,TB} = \Psi_{eq,H} \cdot L_H + \Psi_{eq,V} \cdot L_V + \Psi_{eq,U} \cdot L_U \tag{3}$$

In Equation (3), $\Psi_{eq,H}$, $\Psi_{eq,V}$ and $\Psi_{eq,U}$ are Ψ-values normalized for the building dimensions $L_H$, $L_U$, and $L_V$.

Tables 5 and 6 summarize the equivalent ($\Psi_{eq}$) and average ($\Psi_{avg}$) Ψ-values and coupling coefficients ($L_{2D}$) for the simple and multi-section buildings, respectively. These results provide critical insights into the heat transfer characteristics across the three main building dimensions: height (H) and lengths (V and U).

$$\Psi_{avg,H} = \frac{\sum_{i=1}^{N_H} \Psi_{H_i}}{N_H}$$

$$\Psi_{avg,V} = \frac{\sum_{i=1}^{N_V} \Psi_{V_i}}{N_V}$$

$$\Psi_{avg,U} = \frac{\sum_{i=1}^{N_U} \Psi_{U_i}}{N_U} \tag{4}$$

In Table 5, the vertical dimension of the simple building shows significantly larger average Ψ-values ($\Psi_{avg,V} = -1.051$) compared to the horizontal dimension ($\Psi_{avg,H} = -0.066$), indicating that vertical thermal bridges dominate the overall heat loss contributions. Similarly, Table 6 reveals greater variability in $\Psi_{avg}$ for the multi-section building, reflecting the influence of its complex geometry and material interactions.

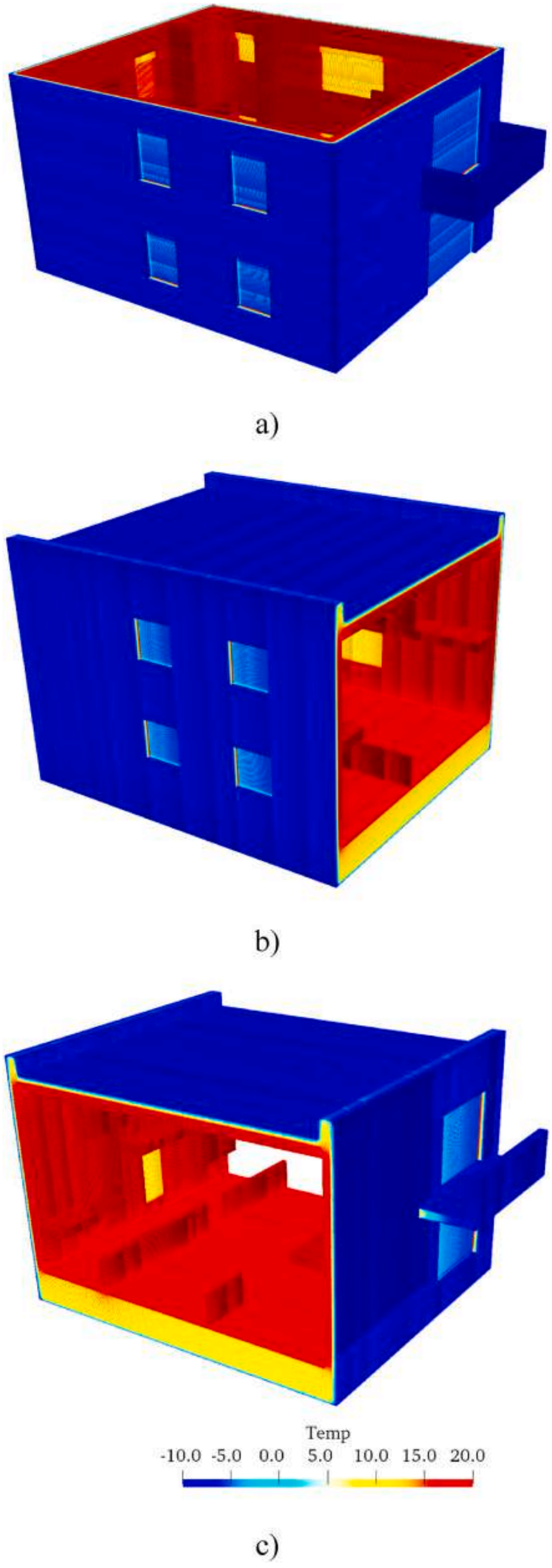


**Fig. 8.** Reconstructed multi-section building from the results of numerical analysis for all cross-sections (section method); a) Horizontal (H), b) Vertical (V) and c) Vertical (U).

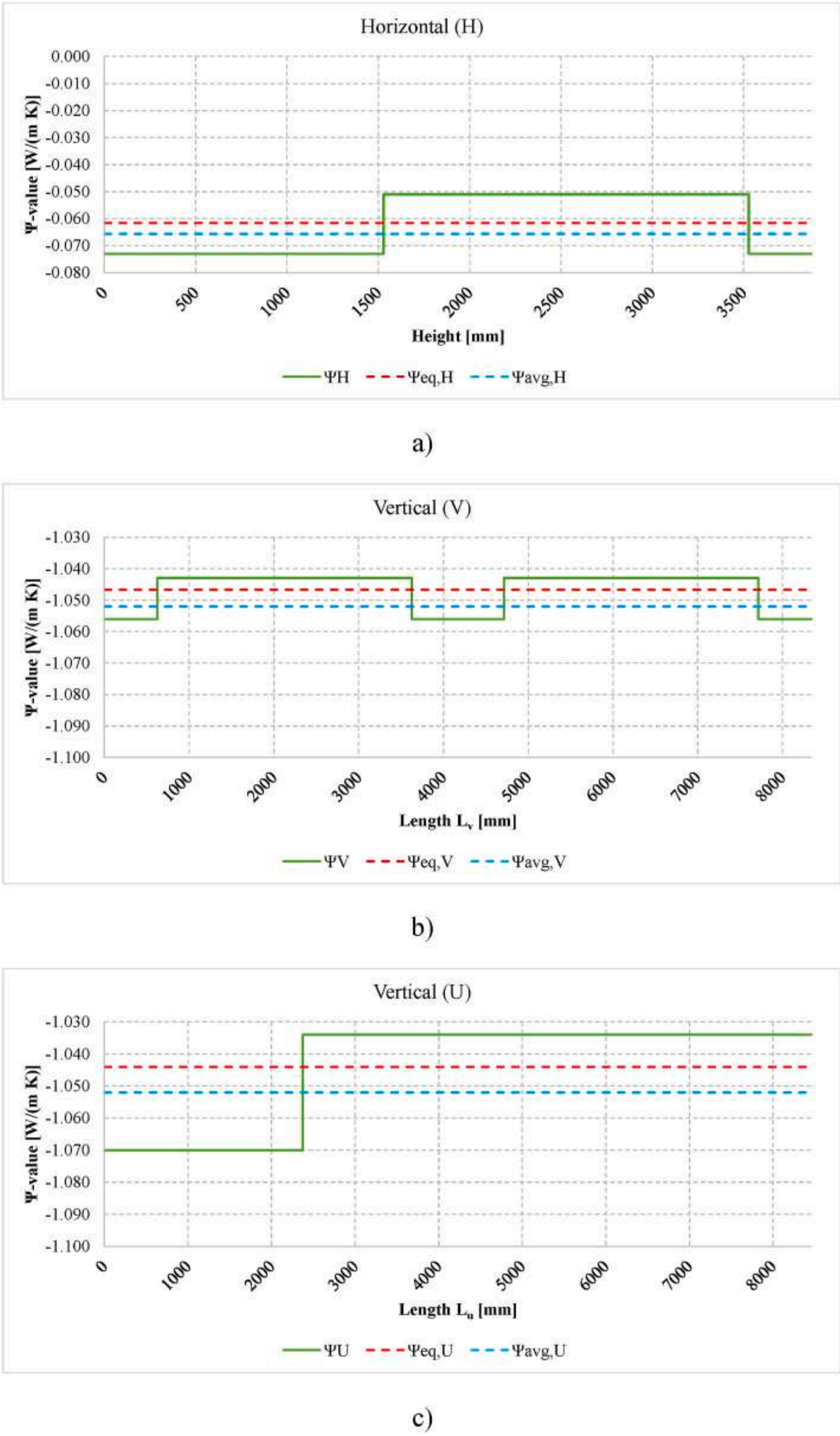


**Fig. 9.** Simple building Ψ-values (section method); a) horizontal, b) and c) vertical.

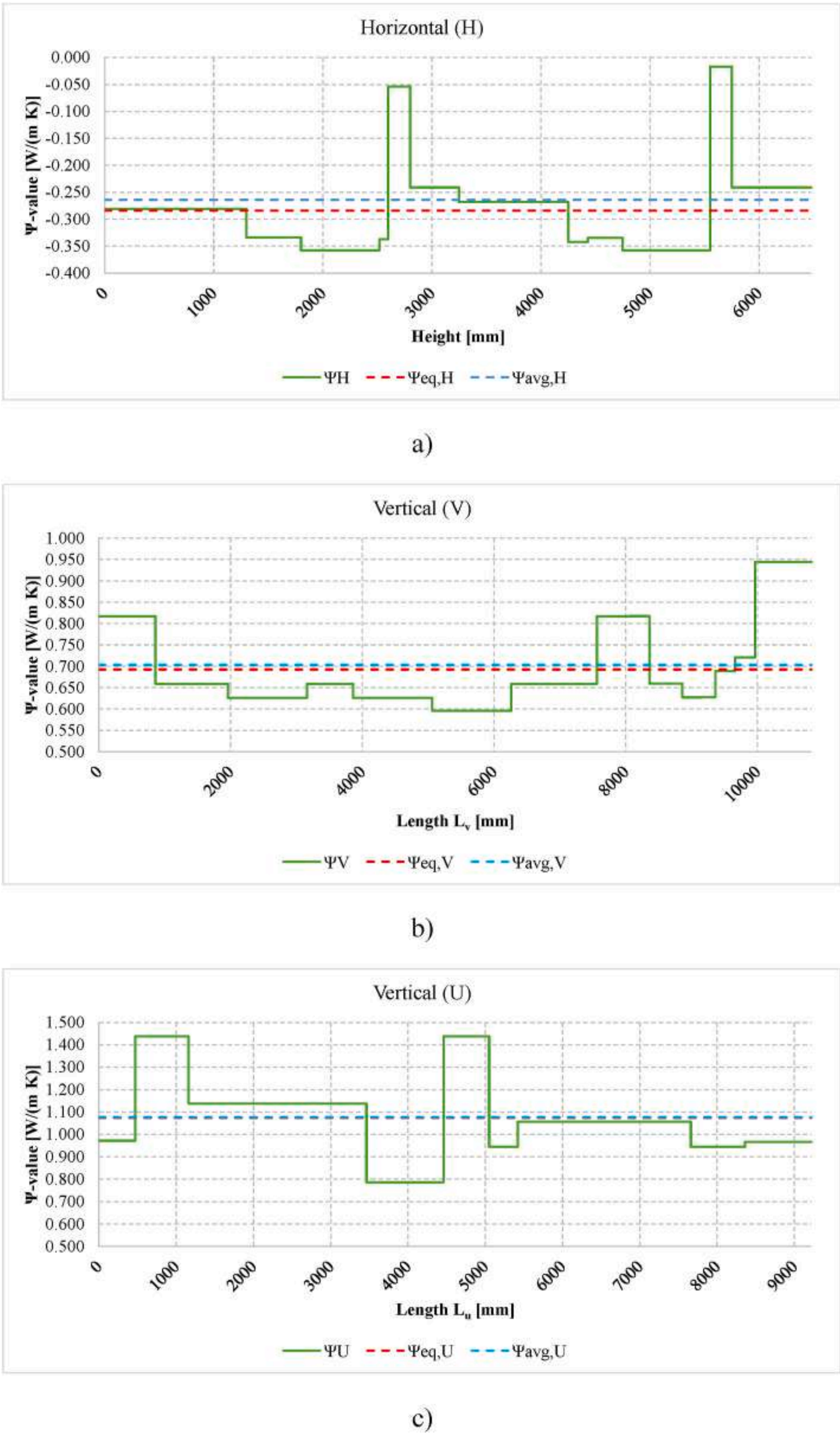


**Fig. 10.** Multi-section building Ψ-values (section method); a) horizontal, b) and c) vertical.

**Table 5**
Equivalent Ψ-values and coupling coefficients $L_{2D}$ (simple building).

| | | | | |
|---|---|---|---|---|
| H | $\sum(\Psi_{Hi} \times L_i)$ | −0.238 | $\sum(L_{2D,Hi} \times L_i)$ | 76.459 |
| | $L_H = 3.8690$ | | | |
| | $\Psi_{eq,H}$ | −0.062 | $L_{2D,eq,H}$ | 19.762 |
| | $\Psi_{avg,H}$ | −0.066 | $L_{2D,avg,H}$ | 18.763 |
| V | $\sum(\Psi_{Vi} \times Li)$ | −8.730 | $\sum(L_{2D,Vi} \times L_i)$ | 60.211 |
| | $L_V = 8.3410$ | | | |
| | $\Psi_{eq,V}$ | −1.047 | $L_{2D,eq,V}$ | 7.219 |
| | $\Psi_{avg,V}$ | −1.051 | $L_{2D,avg,V}$ | 6.638 |
| U | $\sum(\Psi_{Ui} \times L_i)$ | −8.830 | $\sum(L_{2D,Ui} \times L_i)$ | 49.391 |
| | $L_U = 8.4575$ | | | |
| | $\Psi_{eq,U}$ | −1.044 | $L_{2D,eq,U}$ | 5.840 |
| | $\Psi_{avg,U}$ | −1.052 | $L_{2D,avg,U}$ | 5.841 |

H, V, U — Horizontal and vertical sections of the building.
$\Psi_{eq,H}$, $\Psi_{avg,H}$ — Equivalent and average transmittance values for horizontal sections [W/(m K)]
$L_{2D,eq}$, $L_{2D,avg}$ — Equivalent and average thermal coupling coefficient for sections [W/(m K)]
$L_H$ — Total height of the building (m)
$\sum(\Psi_{Ui} \times L_i)$ — Summation of 1D heat transfer contributions.

If all sections are evaluated numerically, as in this work, it is possible to determine the total transmission heat losses ($H_{tr}$) using Equation (5). This calculation accounts for contributions from all cross-sections and provides a benchmark for evaluating the accuracy of the section method. Table 6 compares the total heat losses ($H_{tr}$) with the heat losses due to thermal bridges alone ($H_{tr,TB}$), as calculated using the section method. The difference ($H_{tr} - H_{tr,TB}$) corresponds to the sum of all 1D heat losses.

As shown in Table 7, the simple building exhibits a larger difference between $H_{tr}$ and $H_{tr,TB}$, indicating the dominance of 1D elements in its overall heat transfer. In contrast, the multi-section building shows a smaller difference, reflecting its more complex geometry and the distributed influence of thermal bridges. These ressults validate the section method's ability to accurately estimate $H_{tr,TB}$ using a limited number of cross-sections, supporting the research objective of providing an efficient and practical alternative to detailed numerical analysis as described in ISO 10211 standard.

$$H_{tr} = L_{2D,eq,H} \cdot L_H + L_{2D,eq,V} \cdot L_V + L_{2D,eq,U} \cdot L_U \tag{5}$$

**Table 6**
Equivalent Ψ-values and coupling coefficients $L_{2D}$ (multi-section building).

| | | | | |
|---|---|---|---|---|
| H | $\sum(\Psi_{Hi} \times L_i)$ | −1.839 | $\sum(L_{2D,Hi} \times L_i)$ | 98.810 |
| | $L_H = 6.4800$ | | | |
| | $\Psi_{eq,H}$ | −0.284 | $L_{2D,eq,H}$ | 15.248 |
| | $\Psi_{avg,H}$ | −0.264 | $L_{2D,avg,H}$ | 17.126 |
| V | $\sum(\Psi_{Vi} \times Li)$ | 7.495 | $\sum(L_{2D,Vi} \times L_i)$ | 86.107 |
| | $L_V = 10.8200$ | | | |
| | $\Psi_{eq,V}$ | 0.693 | $L_{2D,eq,V}$ | 7.958 |
| | $\Psi_{avg,V}$ | 0.703 | $L_{2D,avg,V}$ | 7.660 |
| U | $\sum(\Psi_{Ui} \times L_i)$ | 9.909 | $\sum(L_{2D,Ui} \times L_i)$ | 90.208 |
| | $L_U = 9.2200$ | | | |
| | $\Psi_{eq,U}$ | 1.075 | $L_{2D,eq,U}$ | 9.784 |
| | $\Psi_{avg,U}$ | 1.076 | $L_{2D,avg,U}$ | 9.050 |

H, V, U — Horizontal and vertical sections of the building.
$\Psi_{eq,H}$, $\Psi_{avg,H}$ — Equivalent and average transmittance values for horizontal sections [W/(m K)]
$L_{2D,eq}$, $L_{2D,avg}$ — Equivalent and average thermal coupling coefficient for sections [W/(m K)]
$L_H$ — Total height of the building (m)
$\sum(\Psi_{Ui} \times L_i)$ — Summation of 1D heat transfer contributions.

**Table 7**
Transmission heat losses (all cross-sections).

| Building case | $H_{tr,TB}$ [W/K] | $H_{tr}$ [W/K] | $H_{tr} – H_{tr,TB}$ [W/K] |
|---|---|---|---|
| Simple building | −17.799 | 186.062 | 203.861 |
| Detailed multi-section building | 15.564 | 275.125 | 259.561 |

$H_{tr,TB}$ — Total transmission heat losses due to thermal bridges (W/K).
$H_{tr}$ — Total transmission heat losses for the entire building (W/K)

Equation (6) calculates the weighting factors (wi), which quantify the relative importance of each cross-section in contributing to $H_{tr,TB}$.

$$w_i = 100 \cdot \frac{\left|\Psi_{H_i}\right|}{\left|\sum_i \left(\Psi_{H_i}\right)\right|} \ [\%] \tag{6}$$

Table 8 presents the cross-sections with the highest weighting factors ($w_i$), which quantify the relative influence of individual cross-sections on the total heat losses due to thermal bridges ($H_{tr,TB}$). These weighting factors, calculated using Equation (6), help prioritize thermal bridges that have the most significant impact on heat transfer, enabling a more efficient analysis process.

For the simple building, cross-section H001 exhibits the highest weighting factor (57.2 %), despite its length (1.87 m) being slightly shorter than the longest thermal bridge (2.00 m). This is due to its higher Ψ-value, which dominates the heat transfer contribution. Conversely, in the multi-section building, cross-sections such as U03 (2.30 m) dominate the weighting factors due to their combined length and high Ψ-values.

Arranging the weighting factors in descending order highlights the most critical thermal bridges, simplifying the analysis process. These findings validate the section method's capability to focus on key contributors to $H_{tr,TB}$, reducing computational effort while maintaining accuracy. Additionally, the minimal variation in Ψ-values observed in Figs. 9 and 10 supports the trends in Table 8, where the dominance of specific cross-sections is influenced by a combination of Ψ-values and thermal bridge lengths.

The comparison of Ψ-values in Table 8, representing the thermal bridges with the longest lengths, and the equivalent Ψ-values in Table 5 and 6 reveals notable differences. For the simple building, the maximum absolute difference is 17.74 % (cross-section H001), while for the multi-section building, the maximum difference is 5.86 % (cross-section U3). These differences arise because the equivalent Ψ-values in Table 5 and 6 average the contributions of all cross-sections in a given dimension, whereas Table 8 focuses on individual thermal bridges with the longest lengths and highest weighting factors ($w_i$).

When these values are used to calculate the total transmission heat losses due to thermal bridges ($H_{tr,TB}$) using Equation (3), as shown in Table 9, the maximum absolute difference is significantly reduced to just 1.53 % for the multi-section building, despite the 17.74 % difference observed for cross-section H001 in the simple building. This result demonstrates that the section method is effective in balancing these variations and accurately estimating $H_{tr,TB}$, even when individual thermal bridges exhibit significant differences in their Ψ-values.

These findings underscore the robustness of the section method in capturing the overall heat transfer characteristics of a building while simplifying the calculation process. The ability to use a limited number of cross-sections while maintaining accuracy validates the method's practicality and aligns with the research objective of reducing computational effort without compromising performance.

**Table 8**
Maximal weight factors.

| CS name | | Ψ-value | L | w | $L_{max}$ | $\Psi_{Lmax}$ | $w_{Lmax}$ |
|---|---|---|---|---|---|---|---|
| | | W/(m K) | [m] | [%] | [m] | W/(m K) | [%] |
| Simple building | H001 | −0.073 | 1.87 | 57.2 | 2.00 | −0.051 | 42.8 |
| | V02 | −1.043 | 6.00 | 71.7 | 6.00 | −1.043 | 71.7 |
| | U02 | −1.034 | 6.09 | 71.3 | 6.09 | −1.034 | 71.3 |
| Multi-section building | H001 | −0.281 | 1.30 | 19.90 | 1.30 | −0.281 | 19.90 |
| | V02 | 0.659 | 3.10 | 27.26 | 3.10 | 0.659 | 27.26 |
| | U03 | 1.138 | 2.30 | 26.42 | 2.30 | 1.138 | 26.42 |

Ψ-value: Linear thermal transmittance of the thermal bridge [W/(m K)]
L: Length of the thermal bridge (m).
W: Weighting factor of the thermal bridge, indicating its contribution to the $H_{tr,TB}$ (%)
$L_{max}$: Length of the longest thermal bridge in the cross-section (m)
$\Psi_{Lmax}$: Linear thermal transmittance for the thermal bridge with the longest length
$w_{Lmax}$: Weighting factor for the thermal bridge with the longest length

**Table 9**
Comparison of Ψ-value (equivalent Vs. longest length).

| Building case | $H_{tr,TB}$ [W/K] | | \|Diff\| [%] | $H_{tr} - H_{tr,TB}$ [W/K] | | \|Diff\| [%] |
|---|---|---|---|---|---|---|
| | Equivalent | Longest length | | Equivalent | Longest length | |
| Simple building | −17.799 | −17.642 | 0.88 | 186.062 | 179.424 | 3.57 |
| Multi-section building | 15.564 | 15.802 | 1.53 | 275.125 | 273.469 | 0.60 |

$H_{tr,TB}$: Total transmission heat losses due to thermal bridges (W/K)
$H_{tr}$: Total transmission heat losses (W/K)
|Diff| (%): Percentage difference in $H_{tr,TB}$ between the equivalent and longest length calculation

### 3.2. Calculations according to EN ISO 10211

In order to compare the results of the section method, a classic thermal bridge analysis was carried out in accordance with the EN ISO 10211 standard for all thermal bridges that can be located on both the simple and the multi-section building. A total of 13 thermal bridges were identified for the simple building and 30 thermal bridges for the multi-section building.

The results of the numerical analysis are Ψ-values which, multiplied by lengths of the corresponding thermal bridges, give an approximate value for the $H_{tr,TB}$.

After the numerical analysis was done, as with the section method, the results were normalized to show which thermal bridges have the greatest influence on the $H_{tr,TB}$. The weighting factors $w_i$ were also calculated according to Equation (6) and also arranged from the largest to the smallest value (Fig. 10). Normalization was carried out twice in order to bring the sum of the weighting factors $w_i$ to 100 %.

The red line in Tables 10 and 11 shows the limiting factor for the calculation, for which the difference between the $H_{tr,TB}$ calculated using all thermal bridges and a limited number of thermal bridges is less than 5 %. For a simple building this limit is 8 and for a multi-section building 11 thermal bridges, meaning that one has to recognize and numerically calculate at least 8 and 11 thermal bridges, respectively to achieve the difference below 5 %.

It should be emphasized that 8 and 11 thermal bridges are not chosen at random. These thermal bridges have the greatest influence on the $H_{tr,TB}$. In practice, it is very difficult to determine which thermal bridge has the greatest influence, mainly because more than one parameter influences the Ψ-value of thermal bridges: materials, thicknesses, boundary conditions and geometry of the thermal bridge. The Ψ-value is a relative value based on the calculation of 1D transmission heat losses. The dimensions used for these calculations should be known, as these dimensions determine whether the Ψ-value is negative or positive. Another problem with using this method is the fact that a designer does not know where he is with his calculation, as the Ψ-values can be both negative and positive, as can be seen in Fig. 11, and Tables 10 and 11. For example, if only 5 thermal bridges are used to approximate the $H_{tr,TB}$, the error in determining $H_{tr,TB}$ is 12.0 % for a simple building and 34.2 % for a multi-section building compared to the $H_{tr,TB}$ calculated with the effect of all thermal bridges.

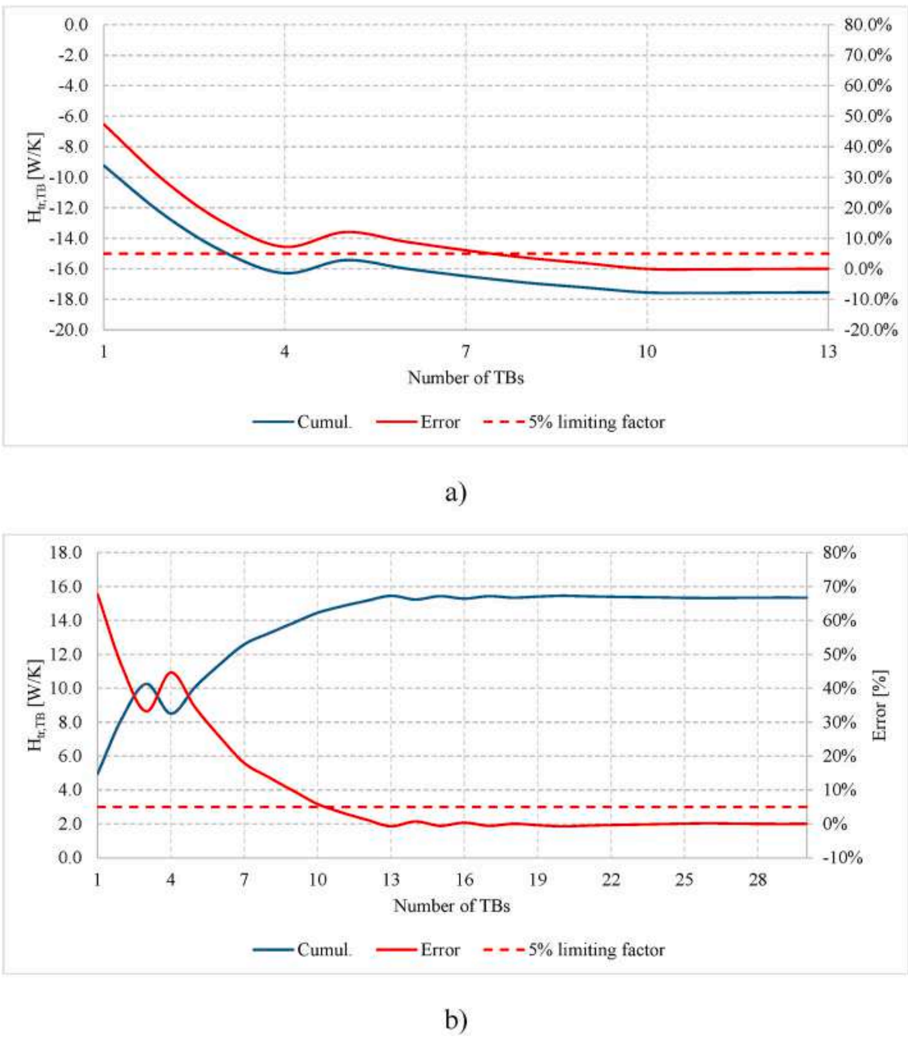


**Fig. 11.** Convergence of the Ψ-value for a calculation according to standard ISO 10211; a) simple building, b) multi-section building.

**Table 10**
Classical analysis according to EN ISO 10211 (simple building).

| # | TB name | Ψ W/(m K) | L m | Ψ × L W/K | w – | $w_{norm}$ – | Cumul. W/(m K) | Error % |
|---|---|---|---|---|---|---|---|---|
| **1** | TM6 | −0.450 | 20.52 | −9.224 | 52.6 | 47.8 | −9.224 | 47.4 |
| **2** | TM8 | −0.457 | 7.08 | −3.239 | 18.5 | 16.8 | −12.463 | 28.9 |
| **3** | TM12 | −0.407 | 6.00 | −2.442 | 13.9 | 12.6 | −14.905 | 15.0 |
| **4** | TM11 | −0.067 | 20.52 | −1.374 | 7.8 | 7.1 | −16.279 | 7.2 |
| **5** | TM2 | 0.110 | 7.74 | 0.853 | 4.9 | 4.4 | −15.426 | 12.0 |
| **6** | TM9 | −0.078 | 7.08 | −0.555 | 3.2 | 2.9 | −15.981 | 8.9 |
| **7** | TM3 | −0.064 | 7.74 | −0.494 | 2.8 | 2.6 | −16.474 | 6.1 |
| **8** | TM13 | −0.071 | 6.00 | −0.428 | 2.4 | 2.2 | −16.903 | 3.6 |
| **9** | TM4 | −0.081 | 4.00 | −0.323 | 1.8 | 1.7 | −17.226 | 1.8 |
| **10** | TM1 | −0.086 | 3.74 | −0.322 | 1.8 | 1.7 | −17.548 | −0.1 |
| **11** | TM10 | −0.003 | 8.34 | −0.024 | 0.1 | 0.1 | −17.572 | −0.2 |
| **12** | TM5 | 0.011 | 2.00 | 0.022 | 0.1 | 0.1 | −17.550 | −0.1 |
| **13** | TM7 | 0.002 | 8.34 | 0.014 | 0.1 | 0.1 | −17.536 | 0.0 |
| | | | **∑:** | −17.536 | 110.1 | 100.0 | | |

| | |
|---|---|
| Ψ | Linear thermal transmittance of the thermal bridge [W/(m K)] |
| L | Length of the thermal bridge (m) |
| Ψ × L | Heat loss through the thermal bridge [W/(m K)] |
| w | Weighting factor, indicating the contribution of the thermal bridge to the $H_{tr,TB}$ |
| $w_{norm}$ | Normalized weighting factor, expressing the relative importance of the thermal bridge |
| Cumul. | Cumulative contribution of the thermal bridges to $H_{tr,TB}$ |
| Error | Cumulative error in estimating $H_{tr,TB}$ due to including only the most significant thermal bridges |

**Table 11**
Classical analysis according to EN ISO 10211 (multi-section building).

| # | TB name | Ψ W/(m K) | L m | Ψ × l W/K | w – | $w_{norm}$ – | Cumul. W/(m K) | Error % |
|---|---|---|---|---|---|---|---|---|
| **1** | TM9 | 0.164 | 30.180 | 4.953 | 32.29 | 24.77 | 4.953 | 67.7 |
| **2** | TM11 | 0.161 | 20.240 | 3.265 | 21.28 | 16.33 | 8.218 | 46.4 |
| **3** | TM29 | 0.295 | 6.890 | 2.035 | 13.26 | 10.18 | 10.253 | 33.2 |
| **4** | TM1 | −0.064 | 27.540 | −1.753 | 11.43 | 8.77 | 8.499 | 44.6 |
| **5** | TM14 | 0.160 | 9.900 | 1.588 | 10.35 | 7.94 | 10.087 | 34.2 |
| **6** | TM25 | 0.400 | 3.300 | 1.319 | 8.60 | 6.60 | 11.406 | 25.6 |
| **7** | TM27 | 0.154 | 7.700 | 1.183 | 7.71 | 5.92 | 12.589 | 17.9 |
| **8** | TM13 | 0.135 | 4.800 | 0.646 | 4.21 | 3.23 | 13.235 | 13.7 |
| **9** | TM23 | 0.476 | 1.280 | 0.609 | 3.97 | 3.04 | 13.844 | 9.8 |
| **10** | TM26 | 0.268 | 2.240 | 0.601 | 3.91 | 3.00 | 14.444 | 5.8 |
| **11** | TM21 | 0.293 | 1.330 | 0.389 | 2.54 | 1.95 | 14.833 | 3.3 |
| **12** | TM28 | 0.096 | 3.380 | 0.324 | 2.11 | 1.62 | 15.157 | 1.2 |
| **13** | TM19 | 0.337 | 0.860 | 0.290 | 1.89 | 1.45 | 15.447 | −0.7 |
| **14** | TM24 | −0.049 | 4.300 | −0.211 | 1.38 | 1.06 | 15.236 | 0.7 |
| **15** | TM30 | 0.191 | 1.000 | 0.191 | 1.25 | 0.96 | 15.427 | −0.6 |
| **16** | TM4 | −0.004 | 36.680 | −0.137 | 0.90 | 0.69 | 15.290 | 0.3 |
| **17** | TM16 | 0.171 | 0.800 | 0.137 | 0.89 | 0.68 | 15.426 | −0.6 |
| **18** | TM6 | −0.073 | 1.180 | −0.086 | 0.56 | 0.43 | 15.341 | 0.0 |
| **19** | TM18 | 0.104 | 0.600 | 0.063 | 0.41 | 0.31 | 15.403 | −0.4 |
| **20** | TM5 | 0.011 | 4.400 | 0.049 | 0.32 | 0.25 | 15.453 | −0.7 |
| **21** | TM3 | −0.002 | 20.360 | −0.032 | 0.21 | 0.16 | 15.421 | −0.5 |
| **22** | TM17 | −0.033 | 0.800 | −0.027 | 0.17 | 0.13 | 15.394 | −0.3 |
| **23** | TM8 | −0.001 | 22.340 | −0.022 | 0.14 | 0.11 | 15.372 | −0.2 |
| **24** | TM10 | −0.001 | 12.680 | −0.019 | 0.12 | 0.10 | 15.353 | −0.1 |
| **25** | TM7 | −0.016 | 1.180 | −0.018 | 0.12 | 0.09 | 15.335 | 0.0 |
| **26** | TM15 | −0.003 | 5.800 | −0.016 | 0.10 | 0.08 | 15.319 | 0.1 |
| **27** | TM20 | 0.003 | 4.320 | 0.014 | 0.09 | 0.07 | 15.333 | 0.1 |
| **28** | TM22 | 0.001 | 9.220 | 0.007 | 0.05 | 0.04 | 15.341 | 0.0 |
| **29** | TM12 | 0.001 | 8.500 | 0.006 | 0.04 | 0.03 | 15.347 | 0.0 |
| **30** | TM2 | 0.000 | 14.360 | −0.006 | 0.04 | 0.03 | 15.341 | 0.0 |
| | | | **∑:** | 15.341 | 130.33 | 100.00 | | |

| | |
|---|---|
| Ψ | Linear thermal transmittance of the thermal bridge [W/(m K)] |
| L | Length of the thermal bridge (m) |
| Ψ × L | Heat loss through the thermal bridge [W/(m K)] |
| w | Weighting factor, indicating the contribution of the thermal bridge to the $H_{tr,TB}$ |
| $w_{norm}$ | Normalized weighting factor, expressing the relative importance of the thermal bridge |
| Cumul. | Cumulative contribution of the thermal bridges to $H_{tr,TB}$ |
| Error | Cumulative error in estimating $H_{tr,TB}$ due to including only the most significant thermal bridges |

Figs. 12 and 13 highlight the thermal bridges with the greatest impact on the total transmission heat losses due to thermal bridges ($H_{tr,TB}$) for the simple and multi-section buildings, respectively as calculated as per EN ISO 10211 standard. These thermal bridges, identified based on their Ψ-values and weighting factors ($w_i$), represent the most critical contributors to overall heat losses.

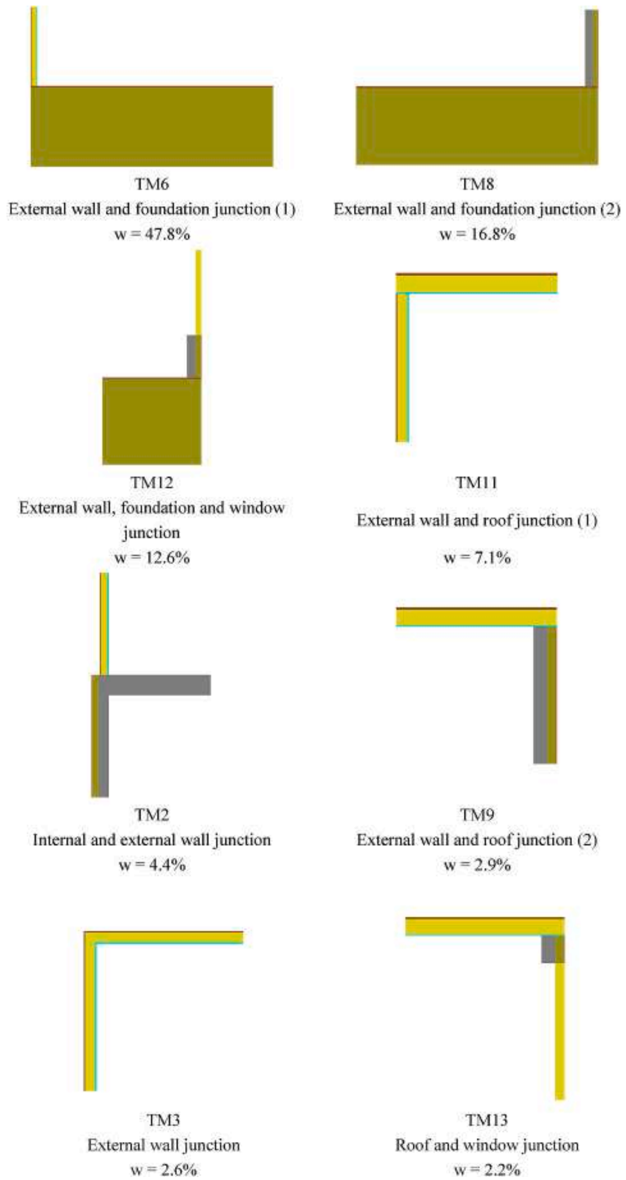


**Fig. 12.** Thermal bridges with the most influence for simple building.

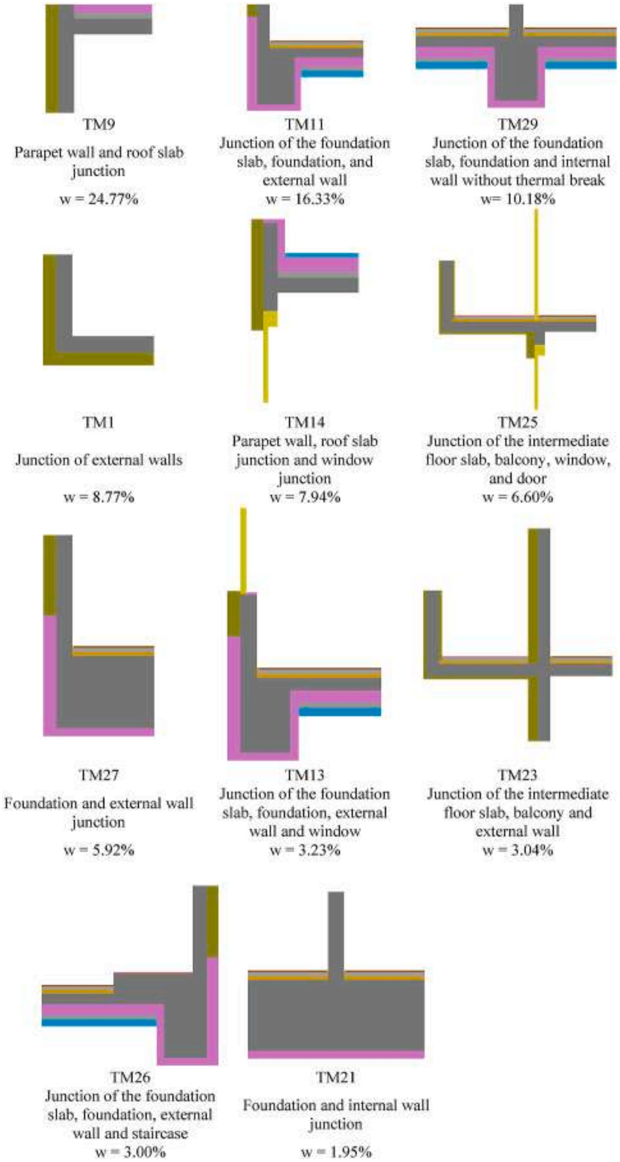


**Fig. 13.** Thermal bridges with the most influence for multi-section building.

### 3.3. Comparison of the section method and the EN ISO 10211 method

This study compared the accuracy, computational efficiency, and practicality of the section method and the EN ISO 10211 method for calculating Ψ-values and transmission heat losses ($H_{tr,TB}$) due to thermal bridges. The results of this comparison are summarized below.

1 Accuracy:

The section method achieved less than 2 % error in estimating $H_{tr,TB}$ compared to the EN ISO 10211 method. Table 12 demonstrates the calculated $H_{tr,TB}$ values for both methods, with differences of 0.88 % for the simple building and 1.53 % for the multi-section building. By contrast, the EN ISO 10211 method showed larger errors due to its reliance on adiabatic surface placement, which does not account for the interaction between nearby thermal bridges. The EN ISO 10211 results were obtained using CRORAL software, which has been validated against benchmark examples provided in the EN ISO 10211 standard. As such, these results serve as reliable references for comparing the performance of the section method. This approach ensures that the accuracy of the section method is validated for thermal bridge analysis.

**Table 12**
Comparison of section method and EN ISO 10211 results.

| Metric | Section Method | EN ISO 10211 Method |
|---|---|---|
| $H_{tr,TB}$ (Simple Building) | −17.799 W/K | −17.642 W/K |
| $H_{tr,TB}$ (Multi-Section) | 15.564 W/K | 15.802 W/K |
| Error (%) (Simple Building) | 0.88 % | – |
| Error (%) (Multi-Section) | 1.53 % | – |
| Number of Cross-Sections | 3 | 13 (Simple), 30 (Multi-Section) |
| Computational Effort | Low | High |
| $H_{tr,TB}$ | Total transmission heat losses due to thermal bridges (W/K) | |
| Error (%) | Percentage difference between the $H_{tr,TB}$ calculated between section method and EN ISO 10211 | |

2 Computational Effort:

The section method requires only three cross-sections (one horizontal and two vertical) to achieve accurate results, significantly reducing computational effort compared to the EN ISO 10211 method, which involves detailed modeling of all thermal bridges. The EN ISO 10211 approach required the identification and modeling of 13 thermal bridges for the simple building and 30 for the multi-section building, resulting in greater time and resource demands.

3 Practicality:

The section method leverages BIM tools, such as Archicad, to streamline the extraction of cross-sections, making it more accessible for designers and engineers. In contrast, the EN ISO 10211 method involves more manual effort in identifying thermal bridges and calculating their lengths, which can introduce errors and inconsistencies.

The results indicate that the section method offers significant advantages in computational efficiency and practicality while maintaining a high degree of accuracy. Its reliance on a minimal number of cross-sections simplifies the modeling process, making it an attractive option for rapid thermal bridge assessments in the early design stages. The EN ISO 10211 method, while precise, is resource-intensive and may not be practical for all projects, especially those with complex geometries.

## 4. Discussion

This study evaluates and compares two methods for calculating Ψ-values of thermal bridges: the section method proposed in this paper and the standardized approach outlined in EN ISO 10211. While both methods aim to quantify thermal bridge effects, the section method simplifies the process by approximating real 3D heat flux through a limited number of horizontal (H) and vertical (V and U) cross-sections. The EN ISO 10211 method, in contrast, involves detailed numerical calculations for all identified thermal bridges, which can be computationally intensive and time-consuming.

The section method achieves its best results when all significant cross-sections are utilized. By calculating Ψ-values for these cross-sections and multiplying them by the corresponding building dimensions ($L_H$, $L_V$ and $L_U$), it provides a streamlined approach to estimating the total transmission heat losses ($H_{tr,TB}$). This eliminates the need to explicitly calculate the lengths of individual thermal bridges, a labor-intensive step in the EN ISO 10211 method.

Tables 5 and 6 demonstrate that both equivalent ($\Psi_{eq}$) and average ($\Psi_{avg}$) Ψ-values provide consistent results across the three primary building dimensions, confirming the reliability of the section method.

The accuracy of the section method is further validated by the results in Tables 7 and 9, which compare $H_{tr,TB}$ values calculated using the section method and the EN ISO 10211 standard. The section method achieves a maximum difference of 3.57 % for the simple building and 0.60 % for the multi-section building when using the longest length approach. In contrast, the EN ISO 10211 method exhibits errors of 40.56 % for the simple building and 6.26 % for the multi-section building, even when all thermal bridges are included. These discrepancies in the EN ISO 10211 results are primarily attributed to the placement of adiabatic surfaces, which fail to account for the interaction effects of nearby thermal bridges.

A key advantage of the section method is its integration with Building Information Modeling (BIM) tools, such as Archicad. These tools streamline the extraction of cross-sections and preparation of models for numerical analysis, significantly reducing the time and effort required for thermal bridge evaluation. This integration makes the section method particularly valuable for early-stage design evaluations, where detailed modeling may not be feasible.

While the section method simplifies the calculation process, the EN ISO 10211 standard still provides valuable insights into the impact of individual thermal bridges. The weighting factors calculated for thermal bridges in Tables 10 and 11 demonstrate the importance of identifying and prioritizing the most critical thermal bridges. For example, the dominant cross-sections identified by weighting factors can guide designers in focusing mitigation efforts on areas with the greatest potential for reducing heat losses. This strategic advantage underscores the complementary roles of both methods: the section method for efficient and broad evaluations, and the EN ISO 10211 method for detailed assessments when required.

The results of this study demonstrate that the section method achieves a practical balance between computational effort and accuracy, making it a viable alternative to the EN ISO 10211 standard. The results validate the proposed formulation by demonstrating its ability to approximate total transmission heat losses with high accuracy and significantly reduced computational effort compared to conventional methods. By focusing on a minimal number of cross-sections and leveraging modern BIM tools, the section method provides an efficient framework for thermal bridge analysis that aligns with the needs of contemporary building design and energy efficiency optimization.

The results shown in this paper validate the proposed formulation by demonstrating its ability to approximate total transmission heat losses with high accuracy and significantly reduced computational effort compared to conventional methods.

## 5. Conclusion

This study introduced a novel approach for calculating Ψ-values of thermal bridges using the section method and compared it to the standardized EN ISO 10211 approach. The section method was developed to simplify the estimation of total transmission heat losses due to thermal bridges ($H_{tr,TB}$) while maintaining high accuracy. By utilizing Building Information Modeling (BIM) tools, such as Archicad, this method allows for the extraction of horizontal and vertical cross-sections, reducing computational effort significantly.

The findings demonstrate that the section method achieves accuracy levels comparable to the EN ISO 10211 approach, with differences in $H_{tr,TB}$ as low as 0.88 % for a simple building and 1.53 % for a detailed multi-section building. Despite its simplicity, the section method effectively minimizes computational resources by requiring only three cross-sections (one horizontal and two vertical) to estimate $H_{tr,TB}$. In contrast, the EN ISO 10211 method involves detailed numerical analysis of all thermal bridges, which can be resource-intensive and impractical for certain projects.

This research highlights the practical advantages of the section method, particularly for projects where computational efficiency is critical. By leveraging BIM integration, the process of cross-section extraction and thermal bridge analysis is streamlined, enabling designers to manage and mitigate heat losses due to thermal bridges more effectively. The study also underscores the importance of simplified numerical approaches in achieving practical and economically viable solutions for building energy efficiency, especially in smaller projects where detailed analysis may not be feasible.

The limitations of the section method lie in its reliance on assumptions regarding cross-section selection and material properties. However, its ability to approximate $H_{tr,TB}$ accurately with fewer computational resources demonstrates its potential for widespread application. Future research will focus on validating the method on buildings with more complex geometries and varying window-to-wall ratios, further refining its applicability to diverse building types.

By bridging the gap between computational efficiency and accuracy, this study contributes to the advancement of thermal bridge analysis techniques, supporting the development of highly energy-efficient buildings.

## CRediT authorship contribution statement

**Mergim Gaši:** Writing – review & editing, Writing – original draft, Validation, Software, Methodology, Formal analysis, Data curation, Conceptualization. **Domagoj Tkalčić:** Writing – review & editing, Visualization, Software, Investigation, Data curation. **Bojan Milovanović:** Writing – review & editing, Supervision, Resources, Project administration, Conceptualization. **Mihaela Maslać:** Writing – review & editing, Visualization, Software.

## Declaration of competing interest

I, Mergim Gaši, hereby declare the following potential conflicts of interest regarding the manuscript titled "Optimizing building energy efficiency: A precise BIM-Based approach for quantifying thermal bridges"

There are no conflicts of interest related to the manuscript. The research was conducted in an impartial manner, and the findings presented in the manuscript are based on objective analysis.

I affirm that the work presented in the manuscript is original and has not been influenced by any conflicts of interest that may compromise the integrity of the research or the publication process. I understand that full disclosure of potential conflicts of interest is necessary to ensure transparency and maintain the credibility of the scientific community.

Should any additional conflicts of interest arise during the review process or after the publication of the manuscript, I commit to promptly informing the journal editor to ensure appropriate actions can be taken.

## Acknowledgements

None.

## Data availability

Data will be made available on request.

## References


[1] L. Pérez-Lombard, J. Ortiz, C. Pout, A review on buildings energy consumption information, Energy Build. 40 (2008) 394–398, https://doi.org/10.1016/j.enbuild.2007.03.007.

[2] F. Ascione, N. Bianco, R.F. De Masi, F. de' Rossi, G.P. Vanoli, Energy refurbishment of existing buildings through the use of phase change materials: energy savings and indoor comfort in the cooling season, Appl. Energy 113 (2014) 990–1007, https://doi.org/10.1016/j.apenergy.2013.08.045.

[3] F. Ascione, R.F. De Masi, F. de Rossi, S. Ruggiero, G.P. Vanoli, Optimization of building envelope design for nZEBs in Mediterranean climate: performance analysis of residential case study, Appl. Energy 183 (2016) 938–957, https://doi.org/10.1016/j.apenergy.2016.09.027.

[4] L. De Boeck, S. Verbeke, A. Audenaert, L. De Mesmaeker, Improving the energy performance of residential buildings: a literature review, Renew. Sustain. Energy Rev. 52 (2015) 960–975, https://doi.org/10.1016/j.rser.2015.07.037.

[5] European Union, Energy performance of buildings directive (EPBD) (EU/2024/1275). https://eur-lex.europa.eu/eli/dir/2024/1275/oj, 2024. (Accessed 1 July 2024).

[6] L. Kempton, G. Kokogiannakis, A. Green, P. Cooper, Evaluation of thermal bridging mitigation techniques and impact of calculation methods for lightweight steel frame external wall systems, J. Build. Eng. 43 (2021), https://doi.org/10.1016/j.jobe.2021.102893.

[7] B.P. Jelle, Traditional, state-of-the-art and future thermal building insulation materials and solutions - properties, requirements and possibilities, Energy Build. 43 (2011) 2549–2563, https://doi.org/10.1016/j.enbuild.2011.05.015.

[8] C.F. Vaz, L.L. Guilherme, F. de, A.C.F. Maciel, A.L. De Araujo, B.B.F. Da Costa, A.N. Haddad, Building information modeling/building energy simulation integration based on quantitative and interpretative interoperability analysis, Infrastructure 9 (2024), https://doi.org/10.3390/infrastructures9050084.

[9] M. Alhammad, M. Eames, R. Vinai, Enhancing building energy efficiency through building information modeling (BIM) and building energy modeling (BEM) integration: a systematic review, Buildings 14 (2024), https://doi.org/10.3390/buildings14030581.

[10] J.P. Carvalho, M. Almeida, L. Bragança, R. Mateus, Bim-based energy analysis and sustainability assessment—application to Portuguese buildings, Buildings 11 (2021), https://doi.org/10.3390/buildings11060246.

[11] D. Tkalčić, B. Milovanović, M. Gaši, M. Jelčić Rukavina, I. Banjad Pečur, Optimization of thermal bridges effect of composite lightweight panels with integrated steel load-bearing structure, Energies 16 (2023), https://doi.org/10.3390/en16186474.

[12] H. Gao, C. Koch, Y. Wu, Building information modelling based building energy modelling: a review, Appl. Energy 238 (2019) 320–343, https://doi.org/10.1016/j.apenergy.2019.01.032.

[13] L. Sanhudo, N.M.M. Ramos, J. Poças Martins, R.M.S.F. Almeida, E. Barreira, M.L. Simões, et al., Building information modeling for energy retrofitting – a review, Renew. Sustain. Energy Rev. 89 (2018) 249–260, https://doi.org/10.1016/j.rser.2018.03.064.

[14] B. Berggren, M. Wall, State of knowledge of thermal bridges-A follow up in Sweden and a review of recent research, Buildings 8 (2018), https://doi.org/10.3390/buildings8110154.

[15] H. Kim, M. Yeo, Thermal bridge modeling and a dynamic analysis method using the analogy of a steady-state thermal bridge analysis and system identification process for building energy simulation: methodology and validation, Energies 13 (2020), https://doi.org/10.3390/en13174422.

[16] P. Santos, M. Gonçalves, C. Martins, N. Soares, J.J. Costa, Thermal transmittance of lightweight steel framed walls: experimental versus numerical and analytical approaches, J. Build. Eng. 25 (2019), https://doi.org/10.1016/j.jobe.2019.100776.

[17] P. Santos, D. Abrantes, P. Lopes, D. Mateus, Experimental and numerical performance evaluation of bio-based and recycled thermal break strips in LSF partition walls, Buildings 12 (2022), https://doi.org/10.3390/buildings12081237.

[18] M. Gaši, B. Milovanović, D. Tkalčić, M.J. Rukavina, Thermal transmittance of a composite lightweight wall panel with integrated load-bearing structure: experimental versus numerical approach, Case Stud. Constr. Mater. 19 (2023), https://doi.org/10.1016/j.cscm.2023.e02631.

[19] P. Santos, G. Lemes, D. Mateus, Thermal transmittance of internal partition and external facade LSF walls: a parametric study, Energies 12 (2019), https://doi.org/10.3390/en12142671.

[20] P. Santos, G. Lemes, D. Mateus, Analytical methods to estimate the thermal transmittance of LSF walls: calculation procedures review and accuracy comparison, Energies 13 (2020), https://doi.org/10.3390/en13040840.

[21] Mergim Gaši, CRORAL, 2024.

[22] International Organization for Standardization, EN ISO 10211: Thermal Bridges in Building Construction – Heat Flows and Surface Temperatures – Detailed Calculations, 2017.

[23] International Organization for Standardization, Building Components and Building Elements – Thermal Resistance and Thermal Transmittance – Calculation Methods (ISO 6946:2017, Corrected Version 2021-12; EN ISO 6946:2017), 2017.

[24] International Organization for Standardization, Thermal Performance of Building Components – Dynamic Thermal Characteristics – Calculation Methods (ISO 13786:2017, Corrected Version 2018-03; EN ISO 13786:2017), 2017.

[25] K. Schild, Wärmebrücken, Springer Fachmedien Wiesbaden, Wiesbaden, 2018, https://doi.org/10.1007/978-3-658-20709-0.